Surface Science 143 (1984) 359–368
North-Holland, Amsterdam

DECOMPOSITION OF ACETIC ACID MONOMER, ACETIC ACID DIMER, AND ACETIC ANHYDRIDE ON Ni(111)

Gregory R. SCHOOFS and Jay B. BENZIGER *

Department of Chemical Engineering, Princeton University, Princeton, New Jersey 08544, USA

Received 8 February 1984; accepted for publication 11 April 1984

The decomposition of acetic acid monomer, acetic acid dimer, and acetic anhydride on Ni(111) were examined by TPD and AES. The monomer decomposed by dehydrogenation to adsorbed acetate; the acetate subsequently decomposed to CO_2, H_2, and adsorbed carbon and oxygen. The dimer decomposed by dehydration to adsorbed acetate, adsorbed methyl, and adsorbed CO. The adsorbed methyl group decomposed to H_2 and adsorbed carbon; the acetate decomposed by the same route as for the monomer though the decomposition kinetics were influenced by the adsorbed CO. Acetic anhydride decomposed at 300 K, with adsorbed acetate, CO, and some methyl groups remaining on the surface. These adsorbates then decomposed to the same products observed for acetic acid dimer. The results show that acetic acid derivatives react by the same mechanism as formic acid derivatives.

In a recent paper, we elucidated the mechanism of formic acid decomposition on nickel under both ultra-high vacuum and moderate pressure conditions [1]. The reaction kinetics determined from surface science experiments were shown to be in agreement with reaction kinetics at moderate pressures when proper accounting was made for formic acid dimerization and adsorbate interactions. In the ultra-high vacuum experiments, it was found that formic acid dimer dehydrated to leave carbon monoxide and formate adsorbed on a Ni(111) surface. Formic acid monomer dehydrogenated on Ni(111) to a surface formate. Adsorbate interactions greatly influenced the decomposition kinetics of the adsorbed formate. Formate–formate interactions were found to be attractive, reducing the reaction rate with increasing coverage. Formate–CO interactions were strongly repulsive, causing a significant acceleration of the decomposition rate with increasing CO coverage. This note reports a UHV study of acetic acid decomposition on Ni(111).

We also investigated the decomposition of acetic anhydride. Anhydride intermediates have been proposed for formic acid decomposition on nickel

* To whom inquiries should be addressed.

0039-6028/84/$03.00

[2–4] and ruthenium [5], and for acetic acid decomposition on nickel [6]. Although one IRRAS study suggested the existence of a formic anhydride intermediate [4], recent EELS studies have found formate [7,8] or acetate [8] intermediates, and no evidence of anhydride intermediates. To our knowledge, the decomposition of anhydrides on nickel has not been investigated. It is important to note that acetic anhydride is normally a stable molecule, whereas formic anhydride is normally unstable. Hence, only acetic anhydride decomposition can be investigated.

The decomposition of acetic acid monomer, acetic acid dimer, and acetic anhydride on a clean Ni(111) surface was studied by temperature programmed desorption (TPD) in a stainless steel ultra-high vacuum system. The mass spectrometer was multiplexed by a computer so that up to five masses could be monitored simultaneously. A constant heating rate of 7.1 K/s was used in all of the experiments. The Ni(111) crystal was characterized by low energy electron diffraction (LEED) and Auger electron spectroscopy (AES). Glacial acetic acid obtained from Sargent-Welch (99.8%) and acetic anhydride obtained from Fisher Scientific Company (98.5%) were further purified by several freeze-pump-thaw cycles prior to using them.

Acetic acid monomer and dimer were prepared by controlling the tempera-

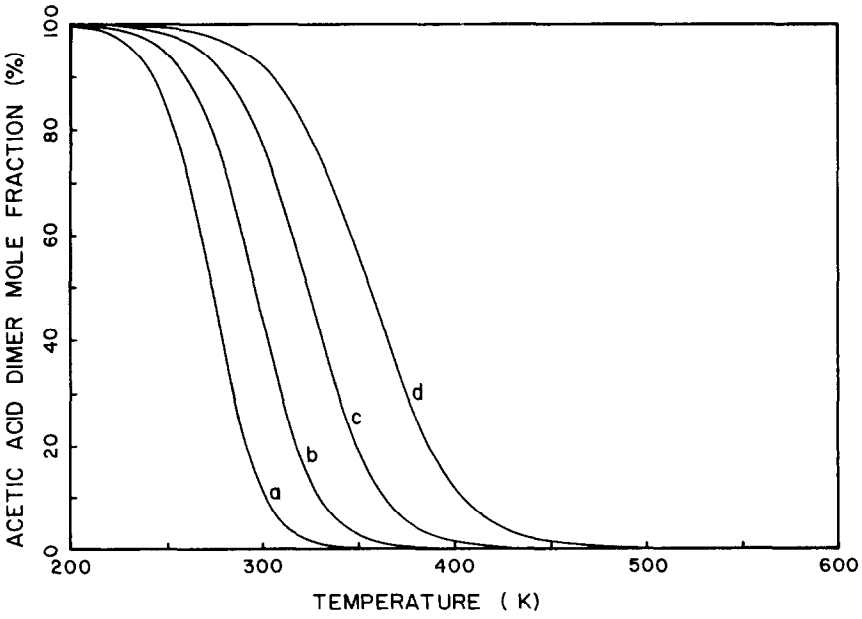

Fig. 1. Extent of acetic acid dimerization in a gaseous mixture of acetic acid monomer and acetic acid dimer. Total pressure: (a) 0.1, (b) 1.0, (c) 10.0 and (d) 100.0 Torr.

ture and pressure of acetic acid in the dosing manifold. The equilibrium constant of acetic acid dimerization, K_d, is [9]:

$$\log_{10} K_d = \log_{10}\left(P_m^2/P_d\right) = 11.789 - 3590/T, \quad (1)$$

where P_m = partial pressure of acetic acid monomer (Torr), P_d = partial pressure of acetic acid dimer (Torr) and T = absolute temperature (K).

Fig. 1 shows the extent of acetic acid dimerization as a function of temperature and pressure. Formic acid behaves similarly; the isobars in fig. 1 are shifted approximately 17 K toward lower temperatures [10]. Nearly all previously reported UHV experiments of acetic acid and formic acid decomposition on metals has occurred under conditions shown in the upper left corner of fig. 1, where the dimer concentration is much higher than the monomer concentration. The possibility of dimerization was neglected in these studies, however. In the present experiments, acetic acid monomer was prepared at a pressure of 160 mT and a temperature of 300 K, and acetic acid dimer was prepared at a pressure of 200 mT and a temperature of 238 K. The acetic acid was admitted into the vacuum system through a 0.2 mm ID tube under conditions of a free jet expansion. Under these conditions the gas will cool and some dimerization of the monomer may occur. Kinetic theory shows that the time between molecular collisions in the gas jet exceeds the transit time of a molecule in the gas jet so that dimerization in the jet may be neglected.

Fig. 2 shows TPD results for decomposition of acetic acid monomer, acetic acid dimer, and acetic anhydride. The scale factors given in fig. 2 refer to the measured mass spectrometer currents. Based on the masses observed, the masses not observed, and the atoms known to be present, we have assigned H_2, CH_3, H_2O, CO, and CO_2 to the $m/q = 2$, 15, 18, 28, and 44 spectra, respectively. For easy comparison, fig. 3 shows the significant differences in the hydrogen ($m/q = 2$) desorption spectra from acetic acid monomer, acetic acid monomer coadsorbed with carbon monoxide, acetic acid dimer, and acetic anhydride.

Fig. 2a shows that hydrogen, carbon monoxide, and carbon dioxide are the primary desorption products from acetic acid monomer decomposition. Trace amounts of water also desorb at 450 K. No hydrocarbon products were observed. Hydrogen desorbs in two peaks. The low temperature peak is typical of hydrogen desorption following hydrogen adsorption on a clean Ni(111) surface [11,12], and has one-third of the area of the high temperature peak. This suggests that acetic acid monomer dehydrogenates upon adsorption to form acetate and hydrogen surface species. The high temperature hydrogen peak coincides with CO and CO_2 desorption. After accounting for the sensitivity of the mass spectrometer, the CO/CO_2 product ratio is 1.6/1. AES revealed that the decomposition reaction left oxygen and carbidic carbon adsorbed on the surface in a coverage ratio of 0.20 ± 0.02.

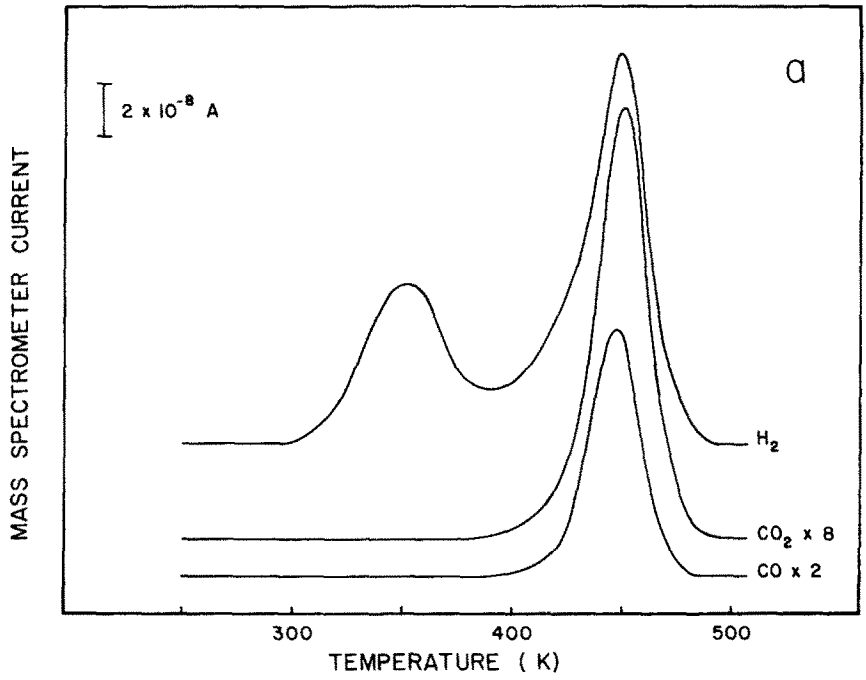
a
2 x 10⁻⁸ A
MASS SPECTROMETER CURRENT
H₂
CO₂ x 8
CO x 2
300
400
500
TEMPERATURE (K)

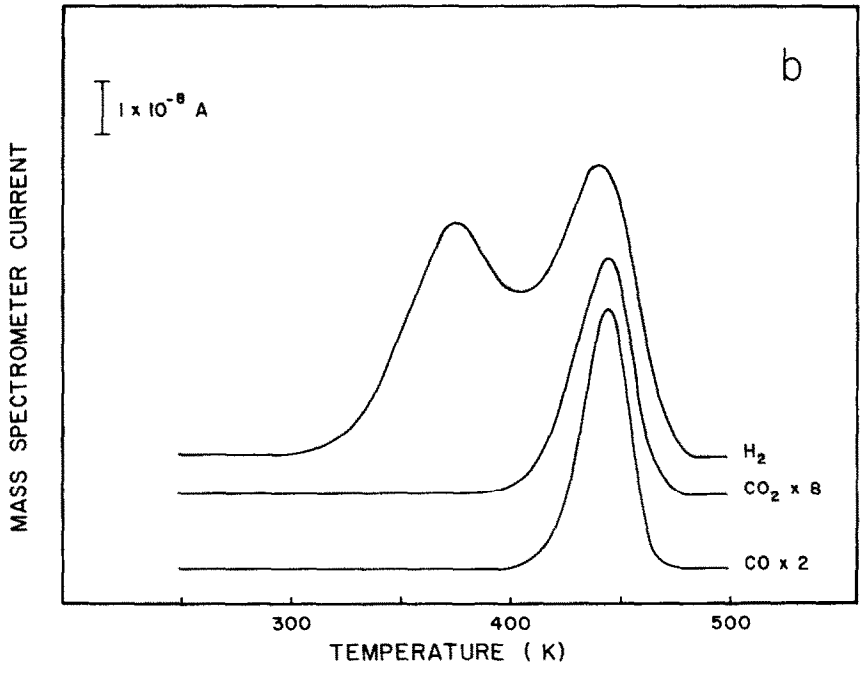
b
1 x 10⁻⁸ A
MASS SPECTROMETER CURRENT
H₂
CO₂ x 8
CO x 2
300
400
500
TEMPERATURE (K)

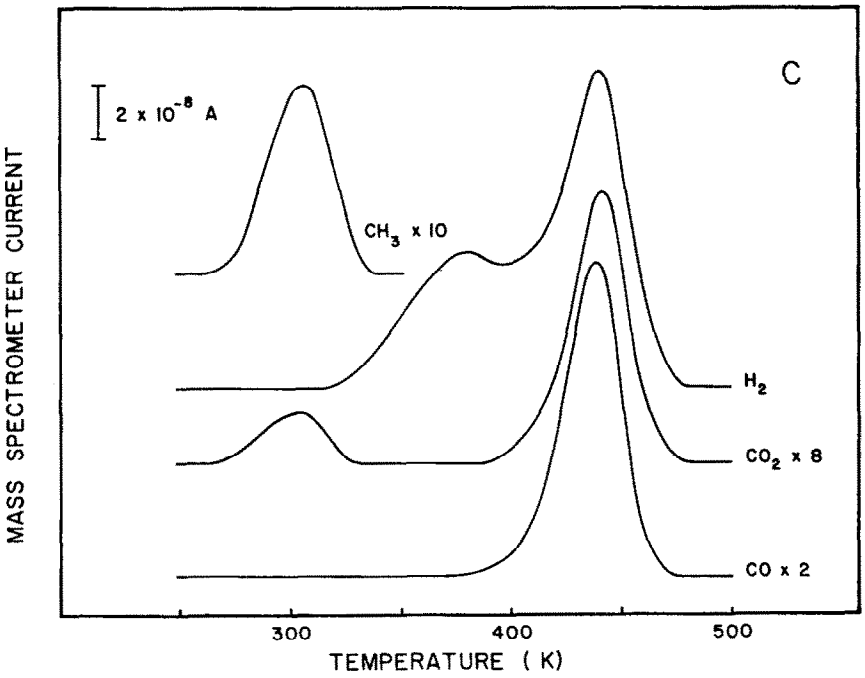

Fig. 2. Product desorption spectra for the decomposition of acetic molecules on Ni(111): (a) acetic acid monomer; (b) acetic acid dimer; (c) acetic anhydride.

The following mechanism is consistent with these results:

$$CH_3COOH_{(g)} \rightarrow CH_3COO_{(ad)} + H_{(ad)},$$

$$2\,H_{(ad)} \rightarrow H_{2(g)},$$

$$CH_3COO_{(ad)} \rightarrow CH_{3(ad)} + CO_{2(ad)},$$

$$CH_{3(ad)} \rightarrow C_{(ad)} + \tfrac{3}{2}H_{2(g)},$$

$$CO_{2(ad)} \rightarrow (1-x)\,CO_{2(g)} + x\,CO_{(ad)} + x\,O_{(ad)},$$

$$CO_{(ad)} \rightarrow CO_{(g)}.$$

Decomposition of the adsorbed acetate is the single rate-limiting step. It is followed by fast secondary reactions. The parameter x represents the fraction of CO_2 which dissociates into adsorbed CO and adsorbed oxygen. The data indicate that some of the adsorbed oxygen and adsorbed carbon combine to form additional CO product.

Fig. 2b shows that hydrogen, carbon monoxide, and carbon dioxide are also the primary desorption products from acetic acid dimer decomposition. No

hydrocarbon products were found, consistent with the observations of previous investigators for acetic acid dimer decomposition on Ni(110) [6]. Trace amounts of water desorb at 450 K. Water also desorbs from formic acid dimer [2,3] and acetic acid dimer [6] at temperatures lower than those which we could obtain. AES indicated that the decomposition reaction left oxygen and carbidic carbon adsorbed on the surface in a coverage ratio of 0.10 ± 0.02. Note that the decomposition of the dimer left less oxygen on the surface than the decomposition of the monomer did. This supports the hypothesis that a low temperature water desorption step occurs. Hydrogen desorbs in two peaks with nearly equal areas. The low temperature peak is typical of hydrogen desorption from an adsorbed hydrocarbon [12,13], which we believe to be an adsorbed methyl group. The high temperature peak coincides with CO and CO_2 desorption. After accounting for the sensitivity of the mass spectrometer, the CO/CO_2 product ratio is 2.7/1.

These results indicate that acetic acid dimer adsorbs and then dehydrates, leaving acetate, CO, and methyl groups adsorbed on the surface. We suggest that the dehydration step proceeds via a proton transfer within the dimer,

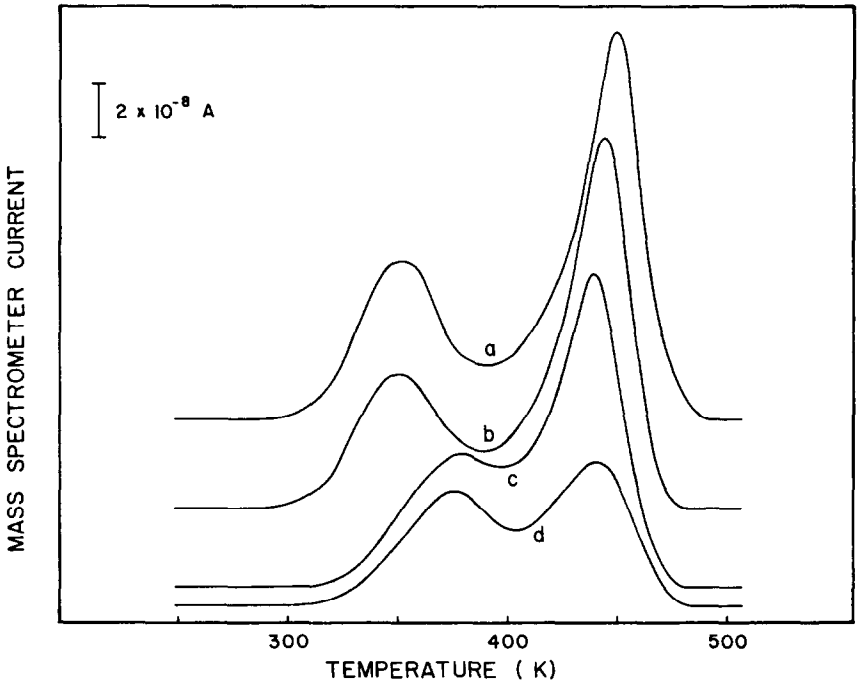

Fig. 3. Hydrogen desorption spectra from the decomposition of acetic molecules on Ni(111): (a) acetic acid monomer; (b) acetic acid monomer with co-adsorbed CO; (c) acetic anhydride; (d) acetic acid dimer.

leading to an adsorbed acetate and a protonated hydroxyl group:

$(CH_3COOH)_{2(g)} \rightarrow (CH_3COOH)_{2(ad)}$,

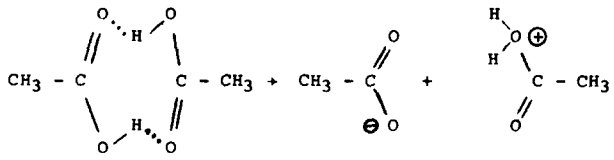

The protonated hydroxyl group then quickly breaks apart into water, which desorbs, while carbon monoxide and CH_3 both remain on the surface. Following decomposition of the adsorbed methyl groups:

$CH_{3(ad)} \rightarrow C_{(ad)} + \frac{3}{2}H_{2(g)}$,

the adsorbed acetates then decompose in a way similar to that observed for acetic acid monomer, but influenced by the presence of CO.

As noted above, other investigators have studied the decomposition of acetic acid on Ni(110) under conditions where acetic acid dimer was the dominant species impinging on the surface [6]. At high coverages, they found an activation energy of 118 kJ/mol and a frequency factor of 6.4×10^{14} s^{-1}. For the decomposition of acetic acid dimer on Ni(111), we estimate an activation energy of 127 kJ/mol and a frequency factor of 4×10^{14} s^{-1}, which agree rather well with their results. The TPD peak widths on Ni(110) were roughly half as wide as those observed on Ni(111), suggesting very strong attractive interactions between adsorbates on the Ni(110) surface [6,8]. Similar differences in peak widths were found for formic acid decomposition on these two surfaces. In addition, the low temperature hydrogen peak on Ni(110) was centered around a much lower temperature than the low temperature hydrogen peak on Ni(111). They thought this peak may have been "the result of adsorption from the background". Water also desorbed below room temperature on Ni(110). We did not observe water desorption below room temperature in our TPD experiments, but mass balances and the AES data suggest that a low temperature water desorption step occurred between dosing and flashing the crystal.

Fig. 2c shows that acetic anhydride decomposes in two steps, and is not an intermediate for acetic acid decomposition. In the low temperature step, CH_3 and CO_2 are the principal desorbed products. The fact that CH_3CO, by far the largest cracking fraction of acetic anhydride, was observed in only trace amounts indicates that this low temperature step is a decomposition step and not an associative desorption step. Hydrogen desorbs in two peaks with unequal areas, also suggesting that acetic anhydride reacts rather than desorbs

molecularly at room temperature. The low temperature hydrogen peak is similar to that observed for acetic acid dimer, and probably results from an adsorbed methyl group. The high temperature hydrogen and CO_2 peaks, and the CO peak are all characteristic of acetate decomposition as discussed above. Trace amounts of water desorb in both steps. After accounting for the sensitivity of the mass spectrometer, the CO/CO_2 product ratio was 3.0/1. AES revealed that the decomposition left oxygen and carbidic carbon adsorbed on the surface in a coverage ratio of 0.12 ± 0.02.

These results suggest that circa 300 K, C–O bond scission of the adsorbed anhydride leads to the formation of a monodentate acetate and an acetyl group. This step is very quickly followed by fast secondary reactions. Most of the acetate adsorbs on the surface, but some leaves as carbon dioxide and CH_3. No acetate was detected by the mass spectrometer. The acetyl groups break apart into adsorbed CO and methyl groups. Some of the methyl groups remain adsorbed on the surface, while others desorb:

$$CH_3COOCOCH_{3(g)} \rightarrow CH_3COOCOCH_{3(ad)},$$

$$CH_3COOCOCH_{3(ad)} \rightarrow (1-y)\, CH_3COO_{(ad)} + y\, CO_{2(g)},$$
$$+ (y+z)\, CH_{3(g)} + (1-z)\, CH_{3(ad)} + CO_{(ad)}.$$

The value of value of y is the fraction of acetate which decomposes into desorbed products; the value of z is the fraction of methyl groups from acetyl groups which leave the surface. Following the decomposition of the adsorbed methyl groups,

$$CH_{3(ad)} \rightarrow C_{(ad)} + \tfrac{3}{2} H_{2(g)},$$

the adsorbed acetates then decompose in a way similar to that observed for acetic acid monomer, but influenced by the presence of CO.

Although 1st order, reaction-limited TPD curves can shift as a function of coverage for a variety of reasons, we have previously shown that adsorbate interactions account for the behavior of formic acid decomposition on nickel [1]. One would expect acetic acid to behave in an analogous fashion. Table 1 indicates the effects of adsorbate interactions on the decomposition kinetics of the adsorbed acetate. Increasing the initial coverage of acetic acid monomer decreases the reaction rate, as indicated by the higher decomposition peak temperature. This is due to attractive interactions between adsorbed acetate molecules, which enhance their stability and raise the activation energy for decomposition. Adsorbed CO–acetate interactions are repulsive, increasing the reaction rate with increasing CO coverage. Hence, co-adsorption of CO with acetic acid monomer decreases the decomposition peak temperature, as does increasing the initial coverage of acetic acid dimer. Fig. 3 clearly shows the destabilizing influence of CO on the hydrogen desorption spectra. We estimate that the magnitude of the CO–acetate repulsive interactions is 3 kJ/mol,

Table 1
Effects of adsorbate interactions on CO_2 desorption peak temperature

Case	Species	Initial coverage	CO_2 desorption peak temperature [a] (K)
1	Acetic acid monomer	0.75	447
	Acetic acid monomer	1.0	452
2	Acetic acid monomer	0.85	445
	with co-adsorbed CO	0.70 [b]	
3	Acetic acid dimer	0.45	448
	Acetic acid dimer	1.0	444

[a] Uncertainty is ± 1 K.
[b] CO coverage is relative to the maximum observed acetic acid monomer coverage.

roughly twice the magnitude of the acetate–acetate attractive interactions.

The underlying physics of the interactions are not clear. Since adsorbed CO and acetate have opposing dipole moments, one might expect the acetate–acetate interactions to be repulsive and the CO–acetate interactions to be attractive if both the CO and the acetate bond perpendicular to the surface. Since the opposite type of interactions are in fact observed, we suggest that the molecules do not adsorb perpendicular to the surface, and/or that factors other than dipole moments contribute to the total interaction energy.

In summary, we have shown that formic acid and acetic acid decompose similarly on Ni(111). Acetic acid monomers dehydrogenate to adsorbed acetate and hydrogen. Acetic acid dimers dehydrate, leaving adsorbed acetate, methyl groups, and CO on the surface. Acetic anhydride decomposes at room temperature, with adsorbed acetate, CO, and some methyl groups remaining on the surface. The decomposition of the adsorbed acetate is influenced by the presence of other adsorbed molecules. Attractive interactions between adsorbed acetate molecules decrease the reaction rate, while stronger CO–acetate repulsive interactions accelerate the reaction rate.

Acknowledgment

We wish to thank the Air Force Office of Scientific Research for their financial support of this work.

References

[1] J.B. Benziger and G.R. Schoofs, J. Phys. Chem., in press.
[2] J.L. Falconer and R.J. Madix, Surface Sci. 46 (1974) 473.

[3] J.B. Benziger and R.J. Madix, Surface Sci. 79 (1979) 394.
[4] M. Ito and W. Suetaka, J. Catalysis 54 (1978) 13.
[5] L.A. Larson and J.T. Dickinson, Surface Sci. 84 (1979) 17.
[6] R.J. Madix, J.L. Falconer and A.M. Suszko, Surface Sci. 54 (1976) 6.
[7] N.R. Avery, B.H. Toby, A.B. Anton and W.H. Weinberg, Surface Sci. 122 (1982) L574.
[8] R.J. Madix, J.L. Gland, G.E. Mitchell and B.A. Sexton, Surface Sci. 125 (1983) 481.
[9] F.H. MacDougall, J. Am. Chem. Soc. 58 (1936) 2585.
[10] A.S. Coolidge, J. Am. Chem. Soc. 50 (1928) 2166.
[11] K. Christmann, O. Schober, G. Ertl and M. Neumann, J. Chem. Phys. 60 (1974) 4528.
[12] G. Dalmai-Imelik and J.C. Bertolini, J. Vacuum Sci. Technol. 9 (1972) 677.
[13] A. Benninghoven, K.-H. Muller, M. Schemmer and P. Beckman, in: Proc. 7th Intern. Vacuum Congr. and 3rd Intern. Conf. on Solid Surfaces, Vienna, 1977, p. 1063.